Light Water Reactor Sustainability Program

Dose Rate Effects on Degradation of Nuclear Power Plant Electrical Cable Insulation at a Common Dose

March 2023

U.S. Department of Energy

Office of Nuclear Energy

Dose Rate Effects on Degradation of Nuclear Power Plant Electrical Cable Insulation at a Common Dose

Muthu Elen[1], Md Kamrul Hasan[1], Donghui Li[1], Yelin Ni[1], Mychal P. Spencer[1], Mark K. Murphy[2], and Andy Zwoster[3], and Leonard S. Fifield[1]

[1]Applied Materials and Manufacturing Group
[2]Nuclear Chemistry and Engineering Group
[3]Advanced Energy Systems Group

March 2023

SUMMARY

The intent of this report is to address an identified knowledge gap in relating accelerated aging of nuclear electrical cables to service aging: dose rate effects (DRE). Here, DRE refer to gamma radiation-induced polymer degradation being a function of dose rate in addition to total absorbed dose. The concern raised is that historical qualification conducted at higher dose rates to simulate service lifetime may underestimate insulation degradation that occurs at lower dose rates in service.

In the work described herein, common nuclear cable insulation materials—cross-linked polyethylene (XLPE) and ethylene propylene diene elastomer (EPDM)—were subjected to accelerated aging at ambient temperature (26°C) at different gamma dose rates of 100, 200 and 1800 Gy/h for select exposure durations to achieve constant total doses of 170, 210 and 300 kGy to evaluate DRE. First, the cable insulation material types investigated are described. Then, the accelerated aging experimental process involving gamma irradiation applied to the insulation specimens at room temperature and different dose rates is discussed. Then, the experimental characterization techniques used to perform this work are elucidated. These include elongation at break (EAB), mass change, yellowness index (YI), carbonyl index (CI), density, indenter modulus (IM), and relaxation constant (τ). Theory of polymer degradation is discussed, and characterization results and discussion are provided. Finally, concluding remarks are made.

The findings from this work and cited prior work reveal that DRE are material dependent, even between similar material categories (e.g., XLPE). In the case of the EPDM studied, degradation of ductility was observed to be greater at higher dose rate for the same total dose, indicating accelerated gamma aging to be more conservative than extended aging. Thus, conclusions regarding the conservatism of historical qualification likely require additional consideration for specific materials and conditions in question.

The results of this study support the contention that, due to inherent limitations and uncertainties associated with prediction of cable remaining useful life from accelerated aging experiments, trending of installed cable insulation health status will be more practical and useful for safe and efficient cable aging management repair and replace decisions than lifetime prediction from historical qualification. The combination of material robustness demonstrated by the qualification process and ongoing monitoring of cable health status combine to provide confidence in continued safe use of existing nuclear cables. Additional research into effective and efficient condition monitoring methods for non-destructive evaluation of installed cables is needed to support aging cable management, including material studies to inform interpretation of measured results.

ACKNOWLEDGEMENTS

CONTENTS

FIGURES

TABLES

ACRONYMS

ATR	attenuated total reflection
CI	carbonyl index
CIE	International Commission on Illumination
CFR	Code of Federal Regulations
CSPE	chlorosulfonated polyethylene
DOE	Department of Energy
EAB	elongation at break
EMDA	Expanded Materials Degradation Assessment (NRC 2014)
EPDM	ethylene-propylene-diene elastomer
EPR	ethylene-propylene rubber
EPRI	Electric Power Research Institute
HEF	High Exposure Facility (at PNNL)
IEC	International Electrotechnical Commission
IEEE	Institute of Electrical and Electronics Engineers
IM	indenter modulus
IPAM	Indenter Polymer Aging Monitor
ISO	International Organization for Standardization
ITE	inverse temperature effects
NIH	National Institute of Health
NPP	nuclear power plant
NRC	Nuclear Regulatory Commission
PE	polyethylene
PNNL	Pacific Northwest National Laboratory
SLR	subsequent license renewal
XLPE	cross-linked polyethylene
XLPO	cross-linked polyolefin
YI	yellowness index

1.   INTRODUCTION

Approximately 20% of the electricity produced in the United States comes from nuclear power plants (NPPs) (Joskow 2006). Originally, NPPs were qualified for an operational lifetime of 40 years (Gazdzinski 1996; Subudhi 1996). As described in the foreword of the U.S. Nuclear Regulatory Commission (NRC) Expanded Materials Degradation Assessment (EMDA) Volume 5: Aging of Cables and Cable Systems, and according to Title 10 of the Code of Federal Regulations, Part 54 (10 CFR 54), Requirements for Renewal of Operating Licenses for Nuclear Power Plants, NPPs can apply for 20-year license extensions following the original 40-year operating period. While most NPPs have entered extended license periods to 60 years, many are considering license extension to 80 years of operation. The viability of a subsequent license renewal (SLR) is dependent upon NPPs operating safely i consistent with the licensing basis established with the original 40-year license. Hence, the NRC has developed aging management program guidance to promote the safe operation of NPPs over license extension periods. The EMDA report identified cable aging-related issues that may be important for the SLR of NPPs.

Based on the issues raised in EMDA Volume 5, a U.S. Department of Energy-sponsored research and development roadmap workshop report (Simmons et al. 2012), and additional emerging issues, Pacific Northwest National Laboratory (PNNL) prioritized a list of 11 cable-aging knowledge gaps focusing on the degradation of cable insulation (Fifield et al. 2018). From this list, four knowledge gaps were selected for investigation as described by Fifield et al., including: (1) inverse temperature effects (ITE) in which degradation due to gamma irradiation is higher at lower temperatures (Przybytniak et al. 2015), (2) diffusion limited oxidation effects due to oxygen permeability hindrance at the polymer surface during accelerated aging (Gillen and Clough 1992), (3) dose rate effects (DRE) where polymer degradation is not only a function of total absorbed gamma dose, but also of the dose rate (Gillen and Clough 1981, 1989), and (4) synergistic effects due to the combined interactions between temperature and radiation (Gillen 2020; Seguchi et al. 2011). Of these four cable knowledge gaps, the focus of this report is on dose rate effects.

Historically, manufacturers qualified electrical cables for 40-years operational lifetime using accelerated aging at temperatures and gamma radiation dose rates well above those experienced by cables in service (Seguchi et al. 2015). The operational lifetimes were estimated based on "equal dose equal damage" assumption where cable polymer degradation is proportional to the total absorbed dose. However, various studies have shown that in some cases the degree of polymer degradation is not only dependent on the total absorbed dose, but also on the dose rate leading to so-called dose rate effects. Gillen et al., studied the effects of dose rate on various cable polymers aged in air environments and determined that more mechanical damage occurred at lower dose rates in some situations (Gillen and Clough 1981). Further exploration of DRE on various cable properties was identified in the EMDA as an outstanding need.

In this study, common nuclear cable insulation materials—cross-linked polyethylene (XLPE) and ethylene-propylene-diene elastomer (EPDM)—were subjected to accelerated aging at ambient temperature (26°C) in the presence of cobalt-60 with different dose rates of 100, 200 and 1800 Gy/h for select exposure durations to achieve a common total gamma dose of 300 kGy to evaluate DRE. The effect of dose rate at ambient conditions was pursued to determine if polymer degradation is dependent on the dose rate without influence of thermal aging. First, in Section 2, the cable insulation material types investigated are described. Then, in Section 3, the accelerated aging experimental process involving gamma irradiation applied to the insulation specimens at room temperature and different dose rates is discussed. In Section 4, the experimental characterization techniques used to perform this work are described. These include elongation at break (EAB), mass change, yellowness index (YI), carbonyl index (CI), density, indenter modulus (IM), and relaxation constant (τ). Section 5 discusses the theory of polymer degradation. Characterization results and discussion are provided in Section 6 and Section 7, respectively. Finally, concluding remarks are made in Section 8.

2. MATERIALS

The materials investigated were selected from those commonly found within nuclear containment to enhance the relevancy of this work (Subudhi, 1996). Both XLPE and EPDM were selected for analysis of DRE effects because insulation material types like these are present within at least 75% of nuclear containments in U.S. NPPs, as shown in Table 1. In addition to the selected material types, low-voltage nuclear grade instrumentation cables were selected because approximately 81% of electrical cables within U.S. NPPs are low-voltage instrument and control cables (Gazdzinski 1996). Furthermore, the investigated materials were extracted from cables produced by three of the most common manufactures of electrical cables for NPPs as shown in Table 1 and Table 2. None of the evaluated materials experienced service aging prior to considerations here.

Table 1. Most common nuclear cable insulation material types found in containment (left) and a sort of the most common manufacturers of cables found within NPPs (right). (Percent of units indicated are approximate values.)

Insulation	Percent of Units (%) (Gazdzinski 1996)	Manufacturer	Insulation	Number of Plants (Gazdzinski 1996)
XLPE	90	Rockbestos	Firewall III XLPE	61
EPDM/EPR	75	Anaconda	EPR	35
SR	27	Brand-Rex	XLPE	30
CSPE	24	Okonite	EPR	26
ETFE	15	Kerite	HTK	25
PVC	7	Rockbestos	Coaxial XLPE	24
PE	3	Raychem	XLPE	23
Neoprene	3	Samuel Moore	EPR	19
Polyimide	3	BIW	Bostrad 7E EPR	19
Polyalkene	2	Kerite	FR EPR	13

XLPE = cross-linked polyethylene; EPDM = ethylene-propylene-diene elastomer; EPR = ethylene-propylene rubber; SR = silicone rubber; CSPE = chlorosulfonated polyethylene; ETFE = ethylene tetrafluoroethylene; PVC = polyvinyl chloride; PE = polyethylene; HTK = high-temperature Kerite; FR = flame retardant.

Table 2. Nuclear grade instrumentation cables used in this report.

Identifier	Manufacturer	Jacket Material	Insulation Material	Jacket Labeling
XLPE-1	RSCC	CSPE	XLPE	2/C 16 AWG COPPER RSCC 600V 90 DEG C WET OR DRY FIREWALL® III SUN RES DIR BUR OIL RES II NEC TYPE TC (UL) FRXLPE SHIELDED CSPE I46-0021
XLPE-2	Brand-Rex	CSPE	XLPE	BRAND-REX XLP/CU POWER & CONTROL CABLE 3/C #10 600V SUN RES XHHW TYPE TC (UL)
EPDM	Samuel Moore	CSPE	EPDM/EPR	Dekoron 2/C 16 AWG 600V

XLPE = cross-linked polyethylene; EPDM = ethylene-propylene-diene elastomer; EPR = ethylene-propylene rubber; CSPE = chlorosulfonated polyethylene.

2.1   Components of As-Received Electrical Cables

Components of the low-voltage nuclear grade instrumentation cables of this report are shown in Figure 1. The white insulated conductors were extracted from the electrical instrumentation cables of Table 2 by first carefully removing the chlorosulfonated polyethylene (CSPE) jackets. A wire stripping tool was then used to score the insulation in 100 mm increments. Afterwards, the exposed conductors were fixed in place with a vise and the insulation removed by gently pulling the insulation from over the conductors. The extracted insulation specimens were 100 mm in length. The tubular cross-sections were measured as 4.74 mm^2 (1.28 ± 0.04 mm inner diameter and 2.79 ± 0.08 mm outer diameter), 10.99 mm^2 (2.5 ± 0.05 mm and 4.5 ± 0.03 mm outer diameter, 4.64 mm^2 (1.35 ± 0.07 mm inner diameter and 2.78 ± 0.04 mm outer diameter) for the XLPE-1, XLPE-2, and EPDM insulations, respectively.

1.   CSPE Jacket
2.   Binder Tape
3.   Copper Ground Wires
4.   Insulation Material – XLPE or EPDM
5.   Conductor
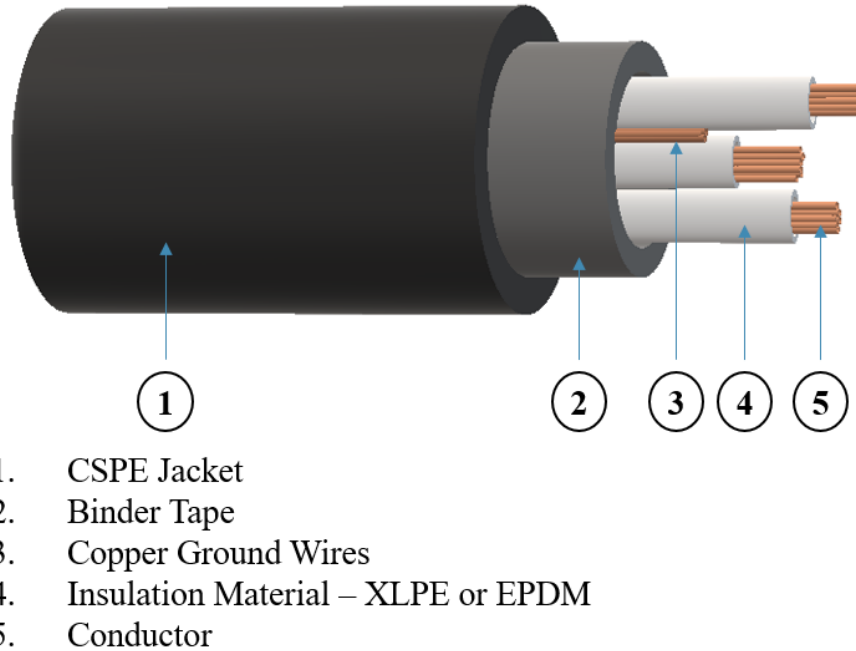
Figure 1. Schematic of low-voltage nuclear grade electrical cables and their exposed components. The insulation material (4) is the polymeric material considered in this report.

The material types of the extracted insulation were confirmed by comparing their absorbance spectra to literature data using Fourier-transform infrared spectroscopy (FTIR). The spectra of the as-received, or unaged, insulation specimens are shown in Figure 2. Due to their chemical structure, methylene absorption (-CH$_2$-) is useful for identification of both XLPE and EPDM. For all materials, strong characteristic methylene asymmetric and symmetric stretching absorbance peaks were measured at 2916 cm^{-1} and 2848 cm^{-1}, respectively (Hu et al. 2016; Amin 2009). In addition, all materials demonstrated characteristic methylene bending modes at 1462 cm^{-1} (scissoring), 1349 cm^{-1} (wagging), and 729 cm^{-1} (rocking), similar to those reported in literature (Kochetov et al. ; Zhao et al. 2007; Tefferi et al. 2019). Absorption was observed for the unaged EPDM specimen at 1050 cm^{-1}, likely due to trans hydrogen atoms on a double bond—an artifact of the vulcanization process (Linnig and Stewart 1958). Furthermore, absorption of trans-substituted (Guadagno et al. 2011) and tri-substituted (Mitra et al. 2006) alkenes were found at 866 cm^{-1} and 808 cm^{-1}, respectively, for the unaged EPDM specimen. While XLPE-1 and EPDM produced weak carbonyl bonds in the range of 1600 to 1720 cm^{-1}, XLPE-2 exhibited strong carbonyl bonds for the as-received specimen. This is because, even though XLPE-1 and XLPE-2 belong to the same material category, there are differences in their proprietary compositions.
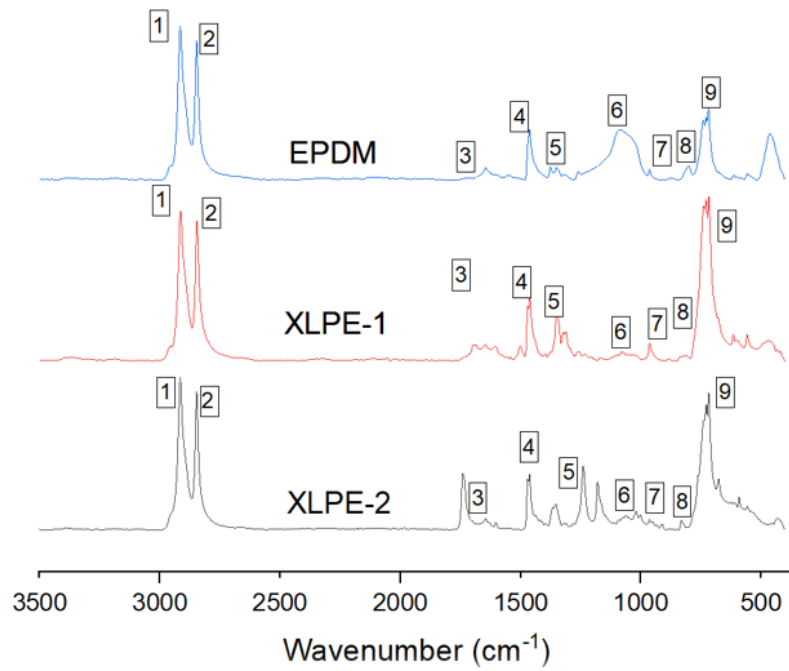
Location	K (cm^{-1})	Functional Groups	Location	K (cm^{-1})	Functional Groups
(1)	2916	CH$_2$ asymmetric stretch	(6)	1050	Trans hydrogen
(2)	2848	CH$_2$ symmetric stretch	(7)	866	Trans-substituted alkene
(3)	1720	C=O stretch	(8)	808	Tri-substituted alkene
(4)	1462	CH$_2$ scissoring	(9)	729	CH$_2$ rocking
(5)	1349	CH$_2$ wagging			

Figure 2. FTIR absorbance of as-received EPDM, XLPE-1, and XLPE-2 insulation material.

3. THERMAL AND RADIATION AGING

Insulation specimens were attached to clips labeled with unique specimen identifiers. The specimens were hung from racks located at controlled positions described in Table 3. To evaluate the effects of DRE, common total absorbed doses were selected, and dose rate was varied for each test condition. Using an approximately 11,000 Ci cobalt-60 sealed source, gamma irradiation was conducted at the High Exposure Facility (HEF) at PNNL (Fifield et al. 2018). With no applied heating, the specimens rack experienced an ambient temperature of 26°C. As-received or unaged specimens were evaluated as reference. For comparison between the test conditions in this report, the dose rates such as 100, and 200 Gy/h are grouped as "low dose rates" whereas the 1800 Gy/h is classified as "high dose rates". Similarly, 90 and 100 kGy are grouped as "low dose", 170 kGy as "intermediate dose" and 300 kGy as "high dose".

Table 3. Evaluated test conditions for exposure of nuclear grade cable insulation specimens.

T (°C)	Total Absorbed Dose (kGy)	Dose Rate (Gy/h)	Materials	Time (hours)	Distance from cobalt-60 Source (cm)
	Unaged	0	XLPE-1, XLPE-2, EPDM	0	-
	90	100	XLPE-1, EPDM	900	91.0
	100	1800	XLPE-1, XLPE-2, EPDM	~56	24.0
26	170	100	XLPE-1, EPDM	1700	91.0
		1800	XLPE-1, XLPE-2, EPDM	95	24.0
	300	100	XLPE-1, XLPE-2, EPDM	3000	91.0
		200	XLPE-1, XLPE-2, EPDM	1500	68.5
		1800	XLPE-1, XLPE-2, EPDM	~167	24.0

4.   EXPERIMENTAL METHODS

To investigate DRE for the selected materials, six characterization methods were employed as discussed below. Tensile and indenter test specimens where conditioned following ASTM D618 Procedure A: at least 48 hours at 23°C ± 2°C and 50% ± 10% relative humidity. Humidity was controlled by placing the specimens within an environmental chamber (Caron Model 7000-25).

4.1   Measurement of Tensile Properties

Following IEC/IEEE 62582-3, tensile EAB was measured for as-received and aged insulation specimens. Table 5 lists the test parameters for each material type. For each test condition, the insulation specimens were cut to a length of 45 mm and the inner and outer diameters were measured using a digital caliper. An ultra-fine tip black permanent marker was used to draw gauge marks centered and at 20 mm separation on the insulation specimens. End tabs of 5 mm length were placed over the ends of specimens with an approximate gap of 2 mm between the ends of specimens and the end tabs (see Figure 4). Different combinations of end tabs and specimen inserts were selected depending on the material type as shown in Table 5. For XLPE-2, thermoplastic polyurethane (TPU) tubing of 5 mm length was used on top of PVC sleeve as end tabs along with insert (EPR insulation with copper wire) to avoid excessive stress in the gripping area. Whereas XLPE-1 required both PVC sleeve end tabs and inserts, the PVC sleeve alone was sufficient for EPDM to avoid specimen breakage in the grip. After attachment of the end tabs and inserts, the specimens were placed centered and along the axis of a pair of pneumatic grips (model #2712-041 for 1 KN load cell) at a separation of 30 mm. A test rate of 10 mm/min was selected for XPLE-1, and 20 mm/min was selected for XLPE-2 and EPDM specimens. A testing rate lower than that specified in IEC/IEEE 62582-3 was used to minimize early failure of specimens. A tensile testing machine (Instron® 3360 Universal Testing System, Norwood, MA) was used to apply tension to the specimens. Elongation at break was estimated for each specimen using videos captured on Nikon D7500 of the specimen deformation. Evolving distance between gauge marks was determined using a PNNL-developed video analysis tool. EAB was calculated as the difference between the final and initial gauge length divided by the initial gauge length for targeted three insulation specimens of each condition, with the average value being reported. Samples that experienced premature failure (e.g., as observed by failure in the grip before tension was applied) were removed from the corresponding data sets, resulting in some scenarios lacking standard deviation information.

Table 5. Test parameters utilized for EAB measurements.

Material Type	Test Rate (mm/min)	End Tab and Insert Material	Grip Pressure (psi)
XLPE-1	10	PVC sleeve and green LDPE insulation with copper wire insert	20
XLPE-2	20	PVC sleeve, TPU tube, and pink EPR insulation with copper wire insert	30
EPDM	20	PVC sleeve	20

XLPE = cross-linked polyethylene, EPDM = ethylene-propylene-diene elastomer, PVC = polyvinyl chloride, LDPE =low-density polyethylene, TPU = thermoplastic polyurethane, EPR = ethylene-propylene rubber
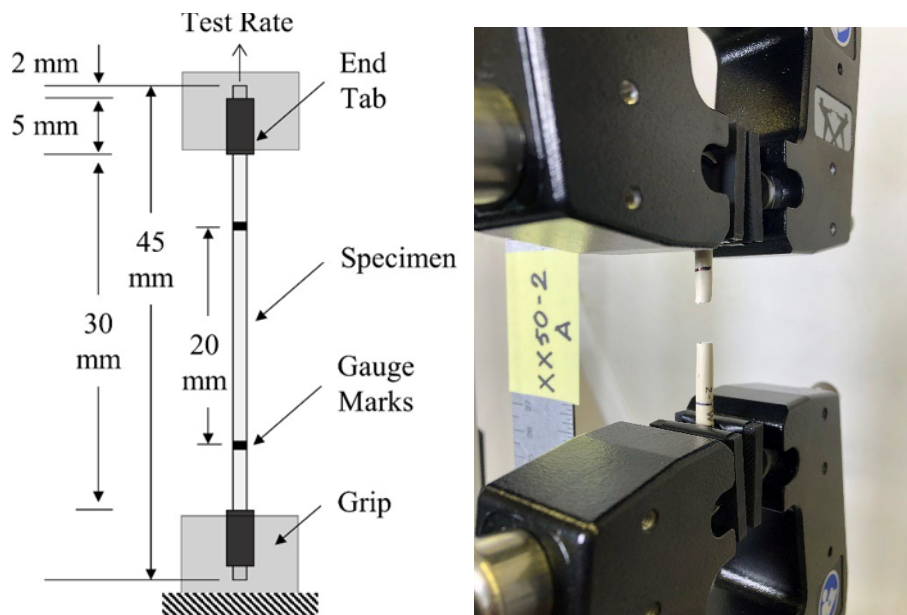
Figure 3. (Left) testing schematic for tensile testing of the insulation specimens and (right) digital image of the test.

4.2   Measurement of Mass Change

Prior work has demonstrated that mass change is a sensitive measure of polymeric degradation. An analytical balance (Fisher Scientific ALF104, ± 0.001 g resolution) was used to measure the mass of the insulation specimens before and after aging. The mass of three insulation specimens was measured for each aging condition, and average mass change was calculated.

4.3   Measurement of Color Change

Polymeric specimens often darken upon aging when exposed to thermal and/or radiative stress. Following ASTM D1729 and ASTM D2244, yellowness index (YI) of aged versus as-received insulation specimens was determined using a light booth (GTI MiniMatcher MM 2e) and digital camera (Nikon D7500). A clamp was used to fix the digital camera in place and orient the camera lens perpendicular to the display plane of the light booth. To optimize the quality of the collected images, the digital camera settings used were as follows: an exposure time of 1/20s to enhance color saturation, an aperture of f/5 to enhance depth of field, and an ISO setting of 100 to reduce background noise. A wireless remote control (Nikon ML-L3) was used to ensure the camera did not move during image collection and to facilitate batch processing. In the light booth, a standard International Commission on Illumination (CIE) D65 light was used and background lighting in the room was extinguished during image collection. To facilitate image calibration and conversion to the CIE XYZ color space, a color reference target was placed on the light booth display plane next to the specimen. To minimize artifacts due to surface reflections from tubular specimens and variations in color along the specimen lengths, each insulation specimen was removed after image collection, rotated slightly, and juxtaposed with the color reference target before another image was captured. This process was repeated twice for a total of three images per insulation specimen.

Due to its components and internal processing, a digital camera and lens will modify the color in digital images in ways inherent to the specific equipment used. It is necessary, therefore, to map these modified colors into a system with an absolute measure of color prior to quantifying color changes in specimens tested. ImageJ (NIH) was used in conjunction with the micaToolbox (Troscianko and Stevens 2015) to

convert the collected image values to CIE XYZ color space. First, the six grey standards located on the bottom row of the color reference target were converted to reflectance values using manufacturer-supplied standard Red Green Blue (sRGB) triplets for each grey standard and then using an iterative least log slope approach (Burns 2017) to convert the triplets to reflectance values. Second, the grey reflectance values were used to create a linear normalized reflectance stack, or calibrated multispectral image, for each collected image. Third, a cone-catch model (Troscianko and Stevens 2015) was generated based upon the charted reflectance spectra of the color reference target. Lastly, the cone-catch model was used to map the linear normalized reflectance stack to the CIE XYZ color space. Calculation of YI for a D65 illuminant is shown in Equation (1), where X, Y, and Z are the evaluated XYZ tristimulus values of the specimen.

$$YI = 100\,(1.2985 \cdot X - 1.1335 \cdot Z)/Y \tag{1}$$

4.4   Measurement of Carbonyl Index

FTIR may be used to identify chemical changes in materials through the tracking of absorption intensities at characteristic absorbance energies. This technique enables determination of the carbonyl index (CI), a measure of the conversion of C-C or C-H bonds to carbonyl (C=O) bonds due to oxidation. In this work, CI was measured to track oxidation occurring in the aging process.

CI measurement was conducted using an FTIR (Bruker Alpha II) equipped with an attenuated total reflection (ATR) attachment. A 10 mm-long sample was extracted from the end of each insulation specimen for the measurement. Individual samples were placed centered on a diamond ATR crystal. For each sample, 64 scans were collected at a resolution at 4 cm^{-1} to minimize signal variation due to random noise. Three replicate measurements were taken per sample. After measurement, the baseline was corrected and analysis of the collected FTIR spectra was performed to calculate the CI. CI was determined as the ratio between the band absorbance intensity of the carbonyl peak (at ~1715 cm^{-1}) ($Abs_{C=O}$) and that of the methylene symmetric stretch peak (between 2846 and 2850 cm^{-1}) (Abs_{C-H}) as shown below in Equation (2).

$$CI = Abs_{C=O}/Abs_{C-H} \tag{2}$$

4.5   Measurement of Density

Density measurement of polymeric materials is important as densification is an indicator of degradation (Subudhi 1996). The density of the insulation specimens was measured following ASTM D792. An approximate length of 5 mm was extracted from the end of the insulation specimens for density measurement. A high-resolution analytical balance (Mettler Toledo™ XPR205, ±0.00005g) was used in conjunction with a density measurement kit (Mettler Toledo™ Density Kit, XPR/XSR-Analytical 30460852) to measure sample mass in air and in water. Prior to immersing the samples, the mass in air was measured. Afterwards, the samples were wetted with isopropanol alcohol to limit formation of air bubbles on the sample surfaces. The samples were then immediately placed in a convex sample holder immersed in deionized water (20.8°C ± 0.3°C); the sample holder was located at a depth of approximately 2.5 cm below the surface. The samples apparent mass was then recorded, and the samples were removed, again wetted with isopropanol, and set aside to dry. The above process was repeated two times for a total of three sets of measurements per insulation specimen (a total of three measurements for each aging condition). The Archimedes principle (water displacement) was used to determine the density (g/cm^3) as shown in Equation (3), where m is the average mass in air (g), m_l is the average mass immersed in water (g), and ρ_l is the density of the liquid (g/cm^3) at the measurement temperature.

$$\rho = m\rho_l/(m - m_l) \tag{3}$$

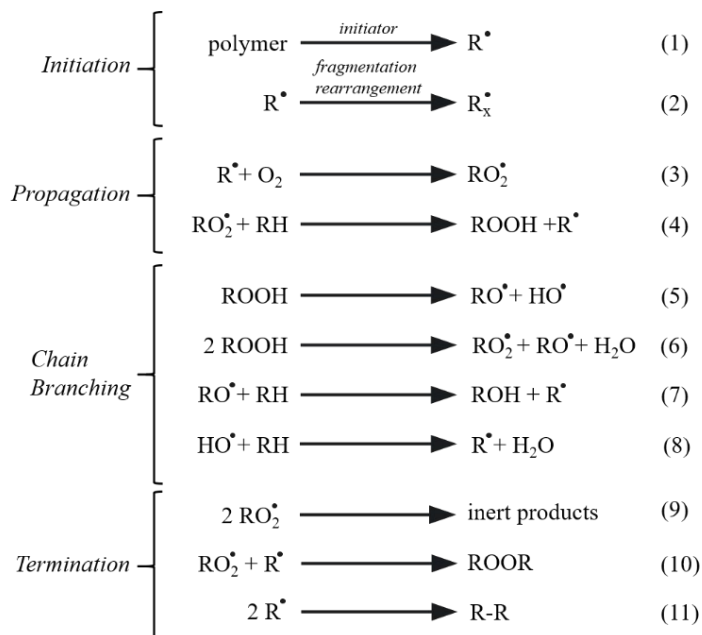## 4.6 Measurement of Indenter Modulus and Relaxation Constant

Indenter modulus (IM) is useful as a metric to track degradation in polymeric materials as it is an indicator of the compressive stiffness of a material, which has been shown to vary with aging. In addition, the relaxation constant (τ) is useful to track the recovery behavior of a deformed polymeric material. The IM of the insulation specimens was measured following IEC/IEEE 62582-2. After pre-conditioning, insulation specimens were placed within a cable clamp assembly of an Indenter Polymer Aging Monitor (AMS Corp. IPAM 4M, Tennessee, USA). The insulation specimens were gently clamped within the IPAM to prevent displacement during measurement. An instrumented probe housed within the IPAM impinged the external surface of the specimens at a displacement rate of 5.1 mm/min to a maximum load of 8.9 N, similar to the recommendations of IEC/IEEE 62582-2. Each measurement was conducted under ambient laboratory conditions (approximately 21°C and 30% relative humidity). The indentation process was controlled, and data collected, through the usage of an external pocket PC. For each insulation specimen, a total of ten indentations were performed at three locations around the specimen circumference while avoiding indentation within 10 mm of each end of the specimen. Per IEC/IEEE 62582-2, the indenter modulus (N/mm) was calculated from the slope of the linear portion of the initial force versus deformation curve as shown in Equation (4), where d_1 and d_2 are the displacements (mm) corresponding to force values of F_1 (1 N) and F_2 (2 N), respectively. In addition to the indenter modulus, the IPAM allows for easy measurement of the insulation specimen relaxation constant, τ. After the maximum load (8.9 N) had been reached during indentation, the probe stopped moving and relaxation of the polymeric insulation was measured over time. The relaxation constant (s) is shown in Equation (5), where F_3 and F_4 are the force (N) values corresponding to measurement times of t_3 (3 s) and t_4 (4 s) after the probe has stopped moving, respectively. The average value and standard deviation of the indenter modulus and relaxation constant was reported after removing the highest and lowest measurement values due to differences in specimen construction, dimensions, and stabilization.

$$IM = (F_2 - F_1)/(d_2 - d_1) \tag{4}$$

$$\tau = |(t_4 - t_3)/ln(F_4/F_3)| \tag{5}$$

5. POLYMER DEGRADATION THEORY

Polymers are ubiquitous in NPP infrastructure. As such, their response to the harsh environments of NPPs has attracted significant interest and been the subject of many studies. There are three primary modes of chemical degradation of polymers in an NPP environment: thermal, radiative, and oxidative. Whenever thermal or radiative degradation occurs in an oxygenated environment these mechanisms become known as thermal-oxidation or photo-oxidation, and oxidative reactions dominate the degradative reaction pathways (Zhang et al. 2020).

$$\text{Initiation} \begin{cases} \text{polymer} \xrightarrow{\text{initiator}} R^{\bullet} & (1) \\ R^{\bullet} \xrightarrow[\text{rearrangement}]{\text{fragmentation}} R_x^{\bullet} & (2) \end{cases}$$

$$\text{Propagation} \begin{cases} R^{\bullet} + O_2 \longrightarrow RO_2^{\bullet} & (3) \\ RO_2^{\bullet} + RH \longrightarrow ROOH + R^{\bullet} & (4) \end{cases}$$

$$\text{Chain Branching} \begin{cases} ROOH \longrightarrow RO^{\bullet} + HO^{\bullet} & (5) \\ 2\,ROOH \longrightarrow RO_2^{\bullet} + RO^{\bullet} + H_2O & (6) \\ RO^{\bullet} + RH \longrightarrow ROH + R^{\bullet} & (7) \\ HO^{\bullet} + RH \longrightarrow R^{\bullet} + H_2O & (8) \end{cases}$$

$$\text{Termination} \begin{cases} 2\,RO_2^{\bullet} \longrightarrow \text{inert products} & (9) \\ RO_2^{\bullet} + R^{\bullet} \longrightarrow ROOR & (10) \\ 2\,R^{\bullet} \longrightarrow R\text{-}R & (11) \end{cases}$$

Scheme 1. Basic auto-oxidation scheme (Gryn'ova et al. 2011).

Most polymers are thought to undergo oxidative degradation under normal conditions by an autocatalytic process known as auto-oxidation. G. Bolland et al. were first to establish the classically understood mechanism of polymer auto-oxidation which has become the contemporary theory. This process is described in several steps including initiation, chain propagation, chain branching, and termination, as shown in Scheme 1 (Gryn'ova et al. 2011). Initiation (Scheme 1, (1)) occurs as weak C-H bonds break, leading to the formation of free radicals (R·). These free radicals can then rearrange (Scheme 1 (2)) without terminating the degradation reaction. Generated radicals quickly react with oxygen to form peroxyl radicals (RO2·) which quickly stabilize into hydro-peroxides (ROOH) through propagation reactions (Scheme 1 (3, 4)). Generated hydro-peroxides can then decompose to form RO· and HO· which results in chain branching reactions (Scheme 1 (5-8)). Generated radicals ultimately form inactive products such as carbonyl groups or unsaturated groups through termination reactions (Scheme 1 (9-11)).

6. RESULTS

In this report, a variety of characterization techniques were employed to assess DRE and to supply more complete information to regulators, operators, and other stakeholders about the long-term operation of nuclear electrical cables. All measurements were compared to those of the as-received specimens.

6.1 Elongation at Break

The relative elongation at break ($\Delta EAB/EAB_i$) of the insulation specimens after aging is compared to that of the unaged insulations specimens in Figure 4. It was observed that both aged XLPE materials at all three dose rates were brittle and degraded below the conservative estimate for insulation lifetime of 50% EAB (Subudhi 1996). On the other hand, the EPDM specimens demonstrated DRE with reduced EAB found at the highest dose rate for all the common dose levels.
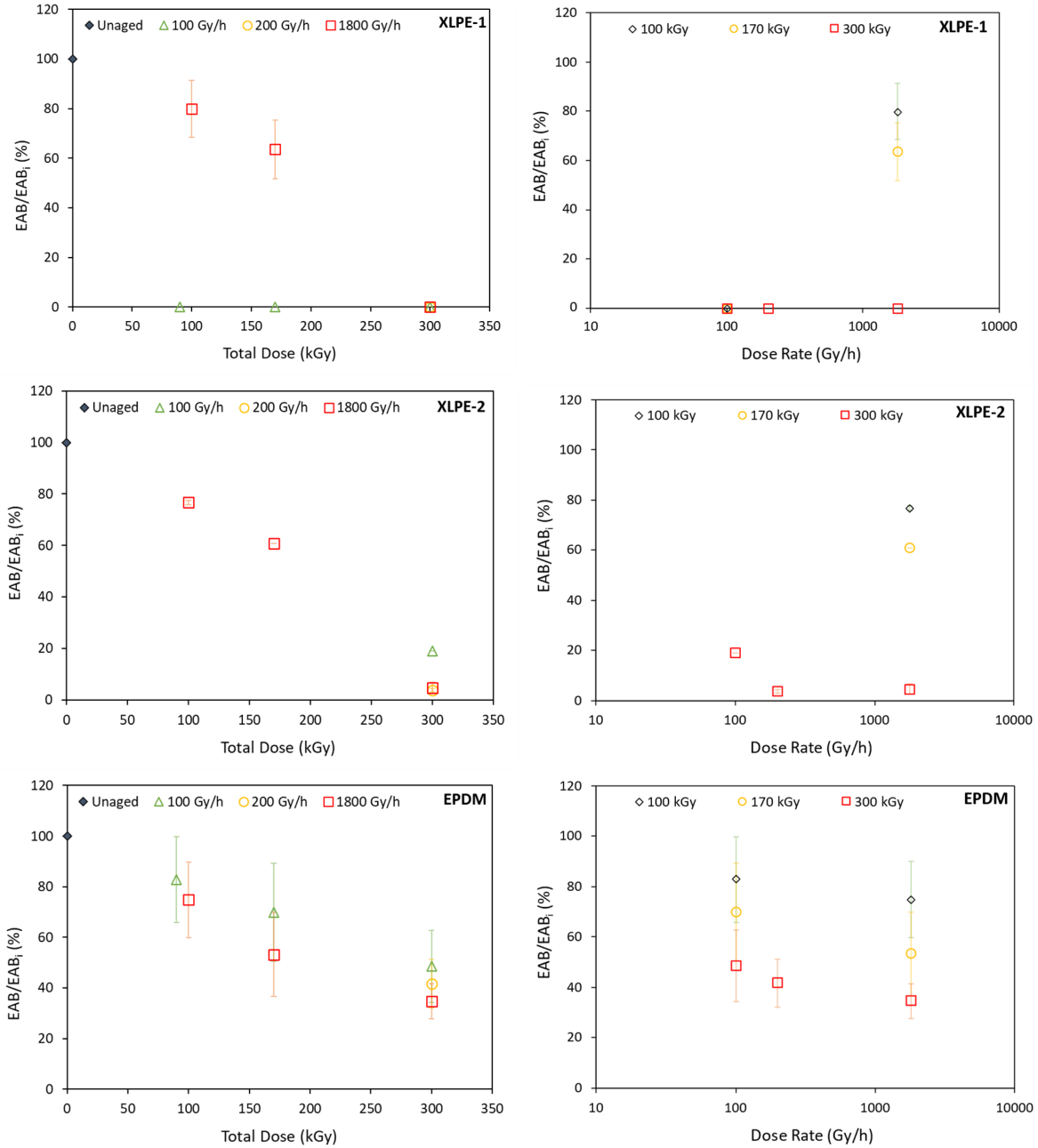
Figure 4. Average relative elongation at break (EAB/EAB$_i$) as functions of total absorbed dose (left) and dose rate (right) for insulation specimens after aging. Error is indicated as one standard deviation. Intermediate absorbed dose specimens for XLPE-2 were not available for testing.

6.2   Mass Change

The relative mass change ($\Delta m/m_i$) of the insulation specimens after aging is compared to that of the unaged insulation specimens in Figure 5. For all materials, a DRE was observed with mass change. Mass change increased with dose rate for EPDM, while it decreased with dose rate for both XLPE materials. It is also to be noted that DRE is observed with mass change for XLPE-1 only at the higher doses and not for lower total absorbed doses.
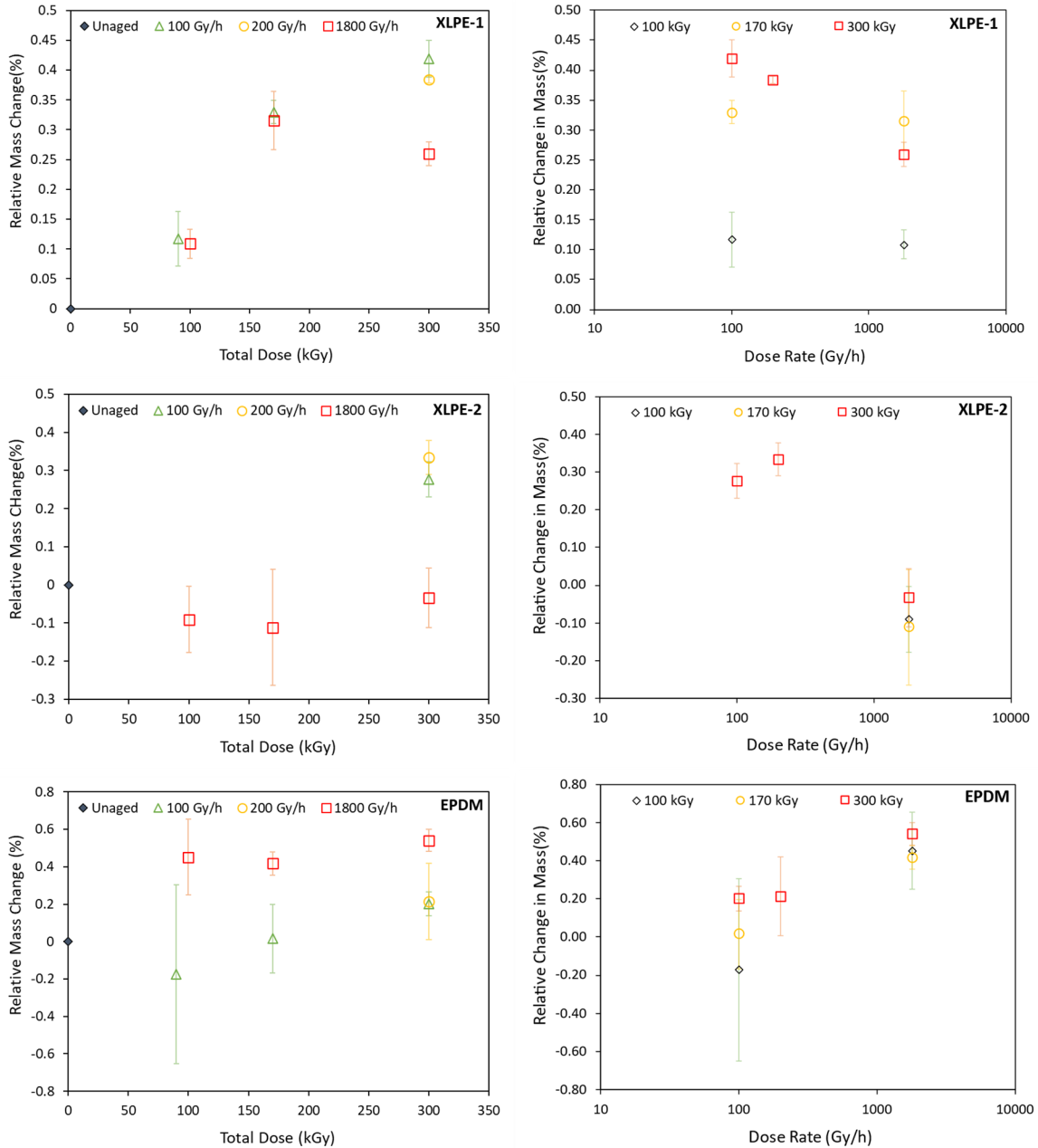
Figure 5. Average relative mass change ($\Delta m/m_i$) as functions of total absorbed dose (left) and dose rate (right) for insulation specimens after aging. Error is indicated as one standard deviation. Intermediate absorbed dose specimens for XLPE-2 were not available for testing.

6.3   Yellowness Index

The relative yellowness index ($\Delta YI/YI_i$) of the insulation specimens after aging is compared to that of the unaged insulation specimens in Figure 6. For all materials, YI increased with respect to the unaged specimen; such yellowing has previously been correlated to the degradation of polymers (Fifield et al. 2022). However, with increasing dose rate it was observed that yellowness index was approximately constant for all materials, indicating YI may not be a sensitive metric for DRE.
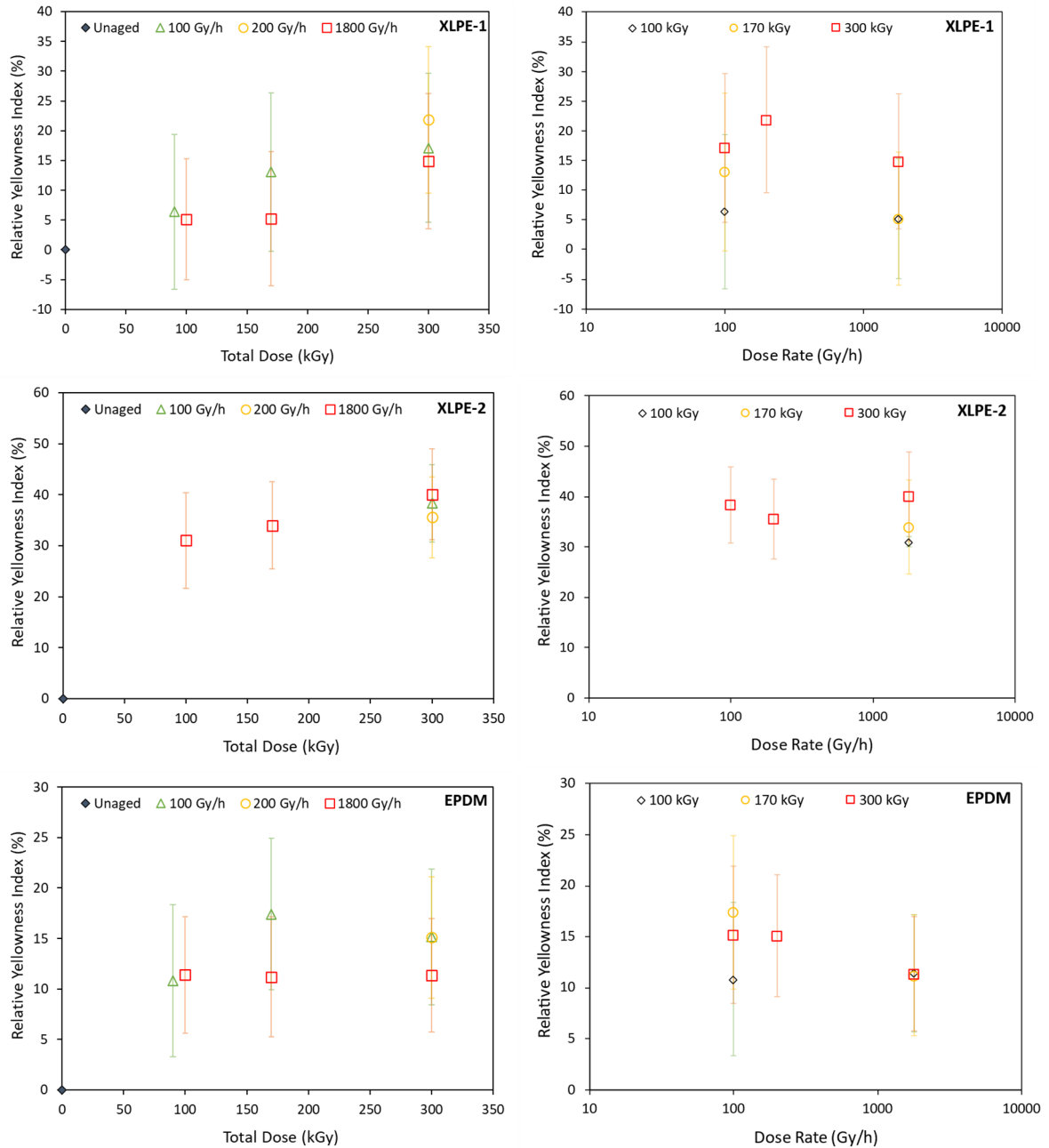
Figure 6. Average relative yellowness index ($\Delta YI/YI_i$) as functions of total absorbed dose (left) and dose rate (right) for insulation specimens after aging. Error is indicated as one standard deviation. Intermediate absorbed dose specimens for XLPE-2 were not available for testing.

6.4 Carbonyl Index

The relative carbonyl index ($\Delta CI/CI_i$) of the insulation specimens after aging is compared to that of the unaged insulation specimens in Figure 8. For the materials investigated, similar trends were found between mass change and carbonyl index. Namely, carbonyl index decreased for XLPE-1, increased for XLPE-2, and decreased for EPDM with increasing dose rate. Therefore, DRE was observed for all materials explored using carbonyl index.
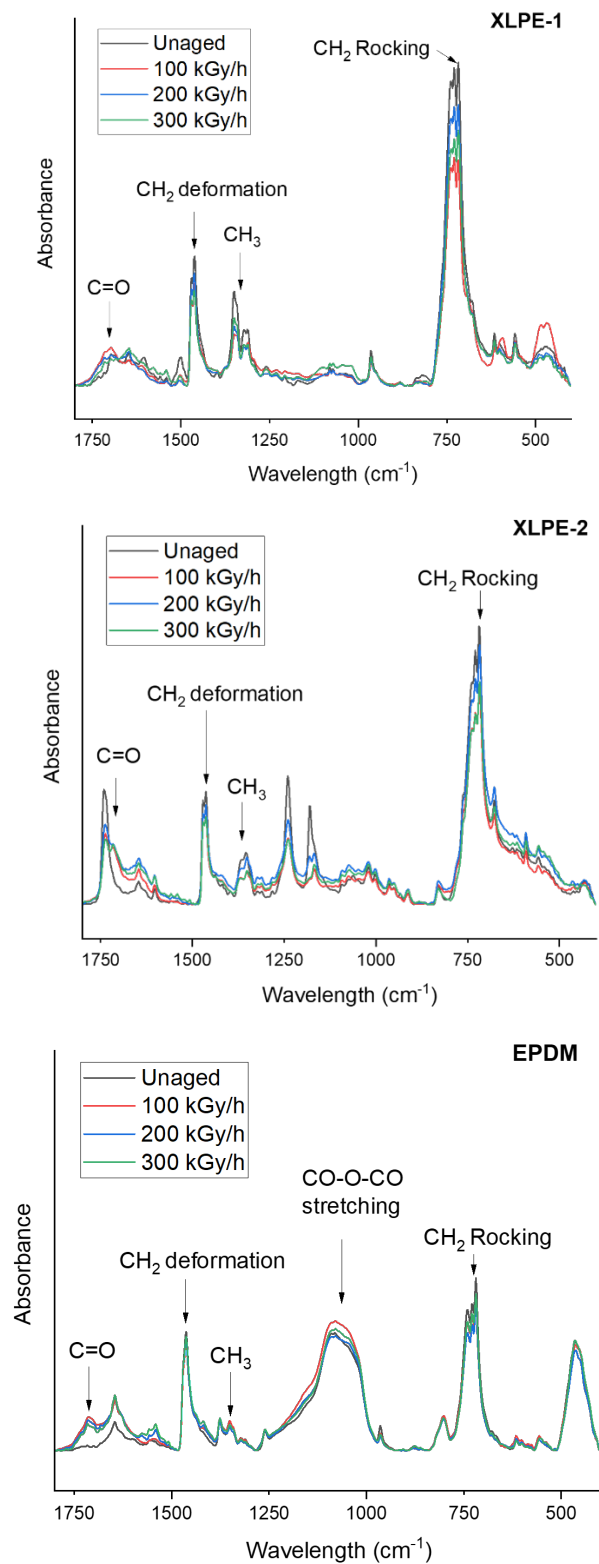
Figure 7. Fingerprint region of FTIR spectra for XLPE-1, XLPE-2 and EPDM respectively.

The fingerprint region of FTIR spectrum, used for analysis of the effects are radiation are between 1800 cm^{-1} to 600 cm^{-1} as shown in Figure 7. For XLPE-1, it is observed that there are differences in peaks at the

carbonyl groups (1650 to 1750 cm^{-1}), -CH$_2$ and -CH$_3$ deformation occurs at ~1462 cm^{-1} and ~1325 cm^{-1} respectively. Significance difference in peaks is also observed at 717 cm^{-1} which refers to the -CH$_2$ rocking behavior in the FTIR analysis. Similar changes in peaks at the same wavelengths are also observed for XLPE-2. For the XLPE-2, there are additional peak differences at 1250 cm^{-1} and 1170 cm^{-1} which are not observed in XLPE-1, and these changes may be due to the presence of additional additives/fillers present in XLPE-2 material, and effect of gamma radiation dose rate in such additives/fillers. In the case of EPDM insulation material, changes are observed at 1650 to 1750 cm^{-1} where the carbonyl groups are, along with CH2 deformation and rocking, and -CH$_3$ deformation occurring at the respective peaks similar to XLPE-1. In additional, there are differences seen at ~1050cm^{-1} for the EPDM where the CO-O-CO stretching occurs (Linnig and Stewart 1958). Figure 8 shows the region of interest between 1710 and 1720 cm^{-1} where the carbonyl groups exist and are used for the calculation of CI. It is observed that at ~1715 cm^{-1}, for XLPE-1 and EPDM, the absorbance is higher at lower dose rate of 100 kGy/h and for XLPE-2, it is lower as compared with the other dose rate insulation spectra. This reflects that oxidation is higher for XLPE-1 and EPDM at lower dose rates, and lower for XLPE-2. Similar behavior have been demonstrated in the literature using FTIR and validated that, it may be due to the cross linking and oxidation occurring at the lower dose rates (Gillen and Clough 1981).
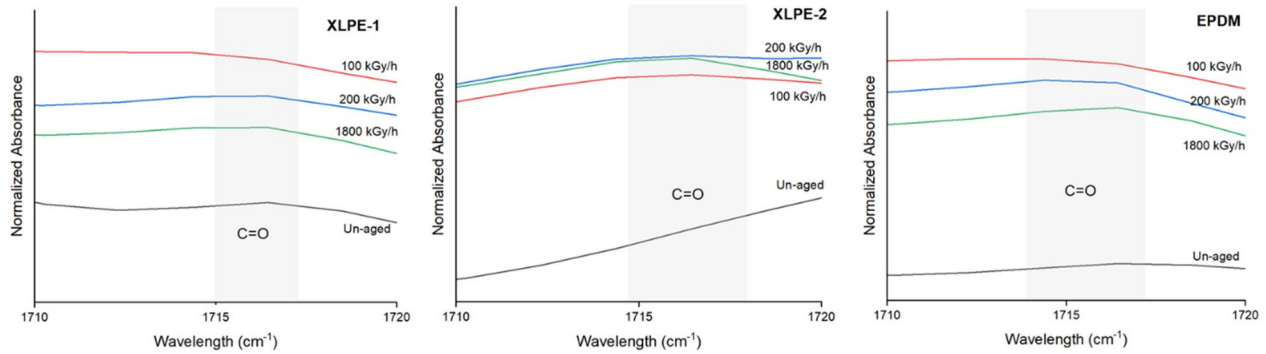

Figure 8: FTIR Absorbance in the carbonyl peak - region of interest between 1710 to 1720 cm^{-1} for XLPE-1, XLPE-2, and EPDM.

Figure 9. Average relative carbonyl index ($\Delta CI/CI_i$) as functions of total absorbed dose (left) and dose rate (right) for insulation specimens after aging. Error is indicated as one standard deviation. Intermediate absorbed dose specimens for XLPE-2 were not available for testing.

6.5 Density

The relative density ($\Delta\rho/\rho_i$) of the insulation specimens after aging is compared to that of the unaged insulation specimens in Figure 8. For the different material types evaluated, density fluctuated within error estimates for all dose rates. Therefore, no DRE was observed with density measurement.
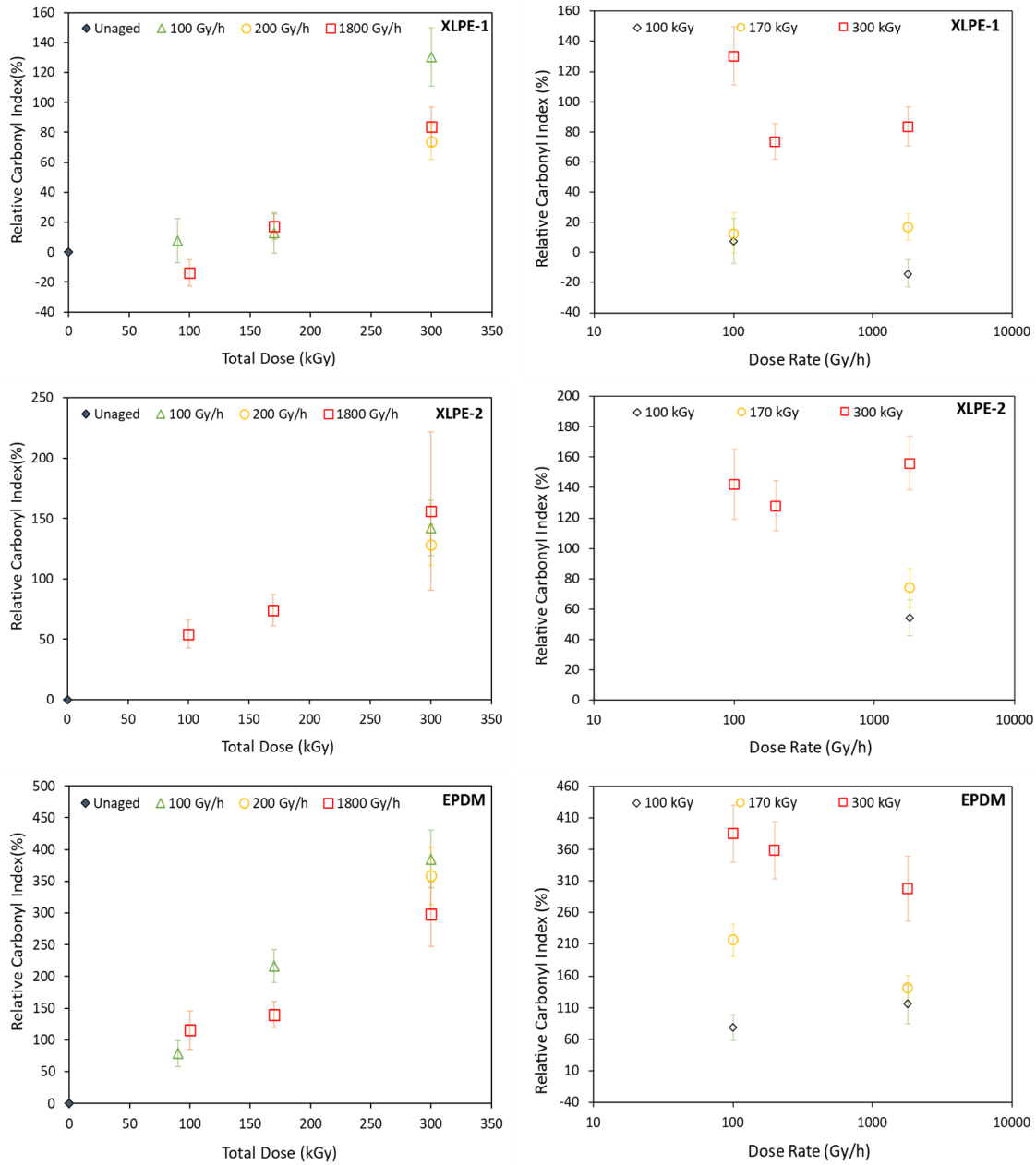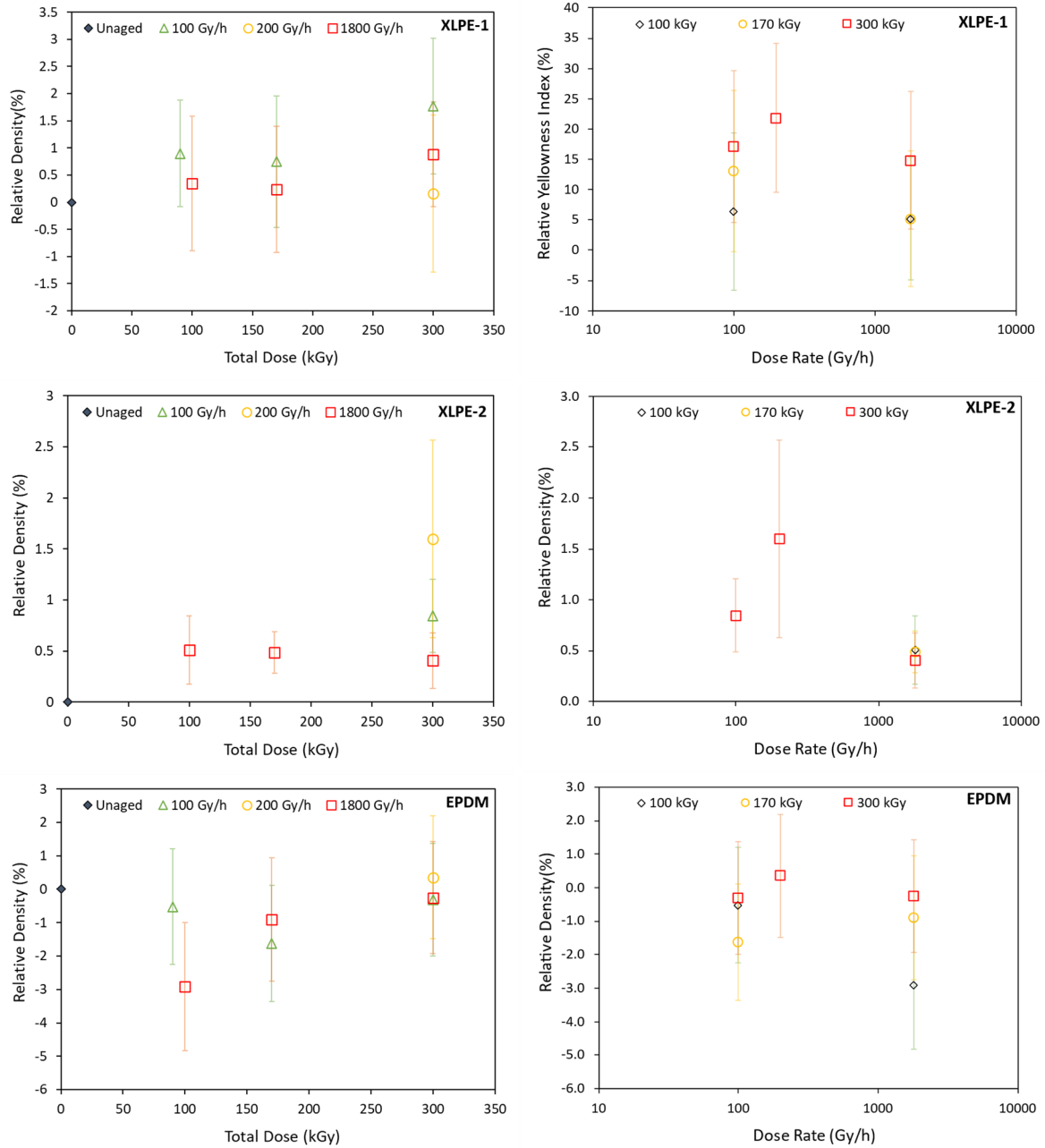
Figure 10. Average relative density ($\Delta\rho/\rho_i$) as functions of total absorbed dose (left) and dose rate (right) for insulation specimens after aging. Error is indicated as one standard deviation. Intermediate absorbed dose specimens for XLPE-2 were not available for testing.

6.6   Indenter Modulus and Relaxation Constant

The relative indenter modulus ($\Delta IM/IM_i$) and relaxation constant ($\Delta\tau/\tau_i$) of the insulation specimens after aging are compared to that of the unaged insulations specimens in Figure 9 and Figure 10, respectively. For similar material types, previous work has shown an increase in IM with total absorbed dose (Fifield et al. 2020). In terms of irradiation temperature, IM was previously found to increase for XLPE and remain constant for EPDM (Fifield et al. 2022).Within error estimates, no variation in IM was observed for the explored materials with dose rate. In addition, in the past, a nearly constant trend was observed for τ with

total absorbed dose, while a decreasing trend was found with increasing temperature (Fifield et al. 2022). In this work, no variation was observed for τ with dose rate. Therefore, no DRE was found using either the indenter modulus or relaxation constant.

Figure 11. Average relative indenter modulus (ΔIM/IM$_i$) as functions of total absorbed dose (left) and dose rate (right) for insulation specimens after aging. Error is indicated as one standard deviation. Intermediate absorbed dose specimens for XLPE-2 were not available for testing.
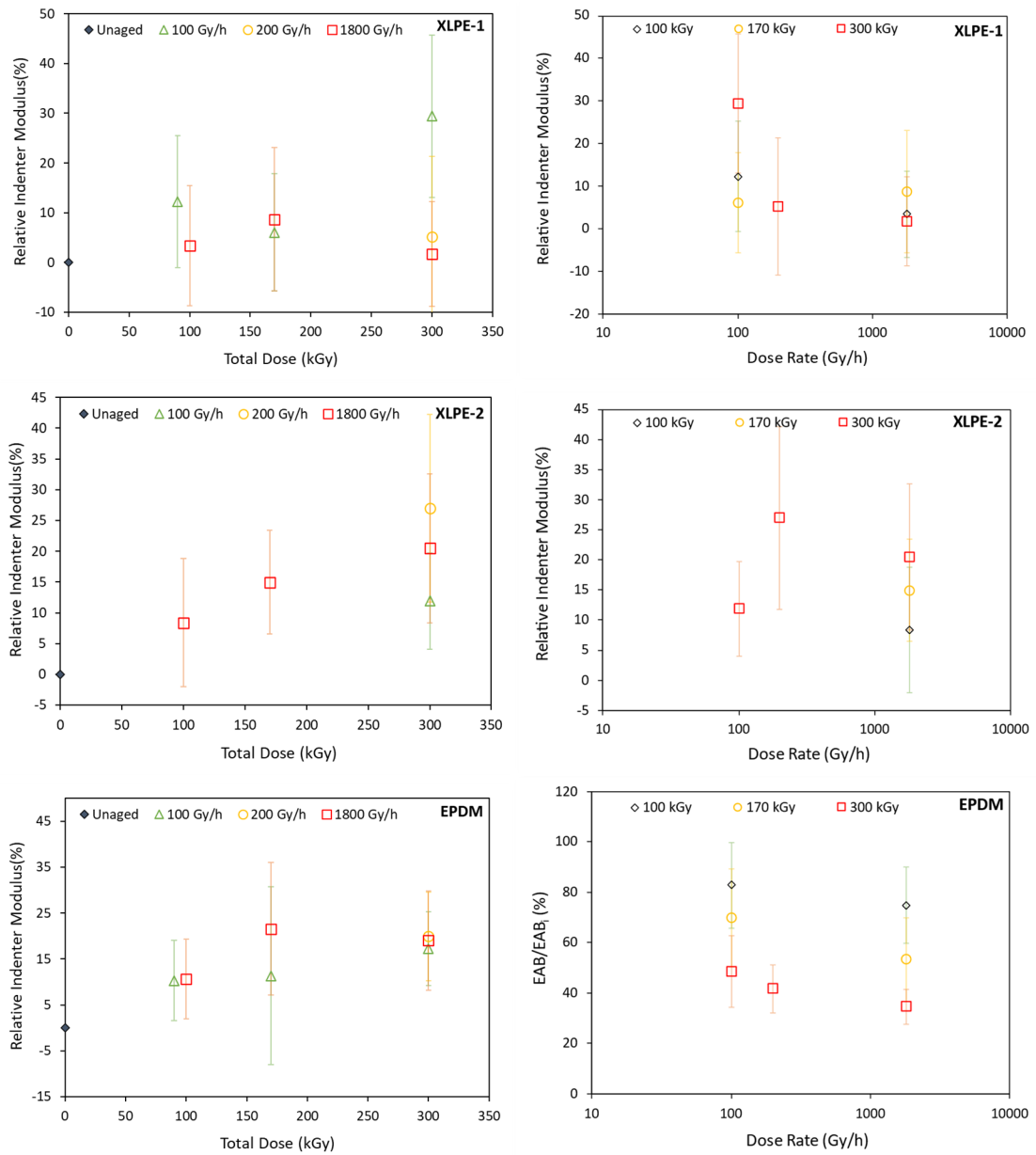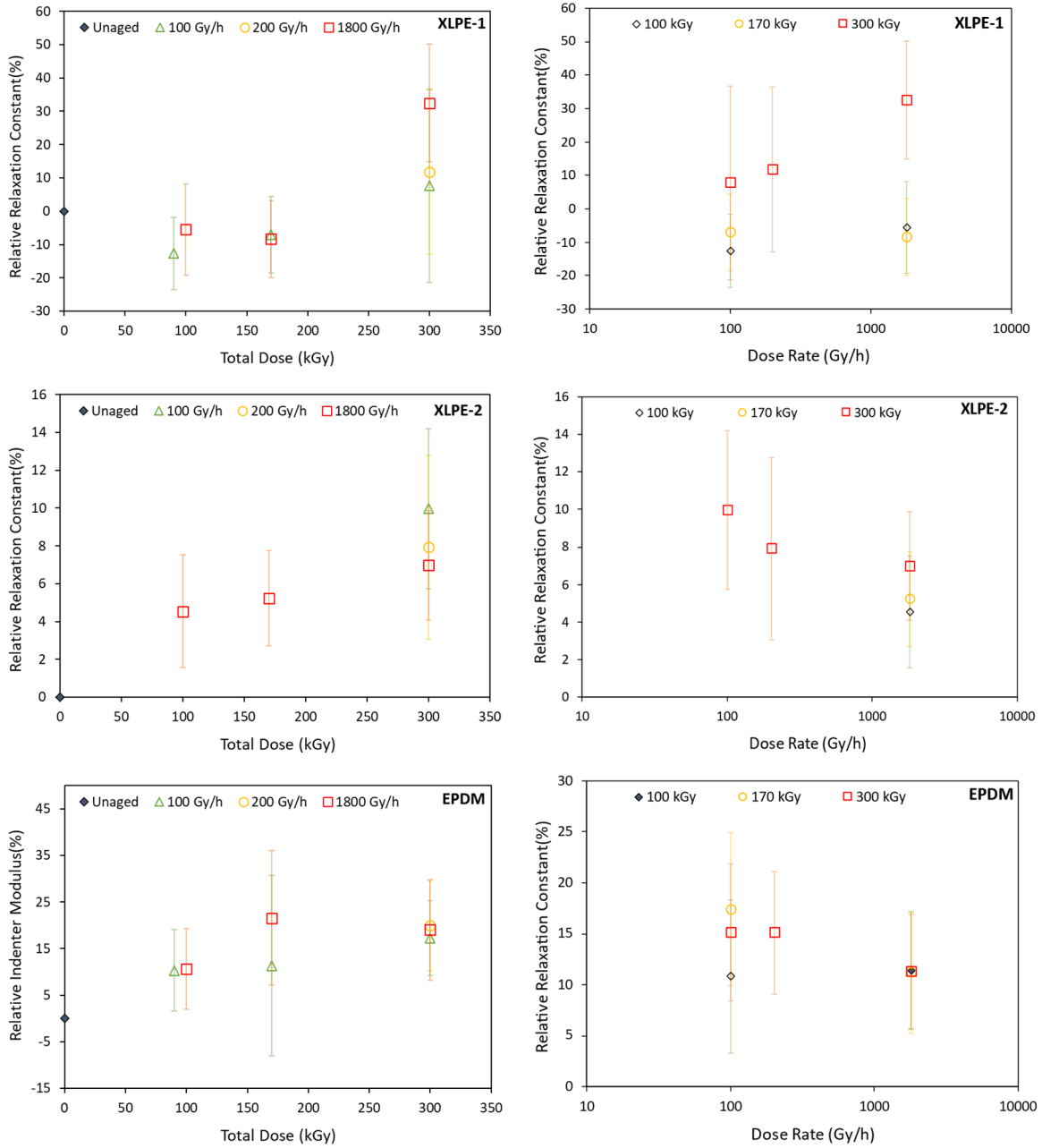
Figure 12. Average relative relaxation time ($\Delta\tau/\tau_i$) as functions of total absorbed dose (left) and dose rate (right) for insulation specimens after aging. Error is indicated as one standard deviation. Intermediate absorbed dose specimens for XLPE-2 were not available for testing.

7. DISCUSSION

Previous work investigating DRE has primarily been conducted at elevated temperatures and under combined thermal and radiative aging. Such work has shown that mechanical damage in electrical cable insulation can be greater at lower dose rates (Gillen and Clough 1981). Investigation into DRE mechanisms for an EPDM composite insulation system revealed increasing dose rates reduced the chain scission process leading to reduced degradation (Sidi et al. 2018). However, previous work has also observed that mechanical, electrical, and chemical property changes of an EPR insulation system were only dependent upon total absorbed dose and not dose rate (Gong et al. 2019). Therefore, additional research was needed, particularly at ambient conditions, to determine the presence of DRE for common NPP electrical cable insulation and its impact on historical qualification.

The focus of this study was the investigation of DRE at ambient conditions to a common dose for three typical NPP electrical cable insulation materials: XLPE (RSCC), XLPE (Brand Rex) and EPDM (Samuel Moore). Based upon the results of this study, tensile elongation at break, mass change, and carbonyl index were found to be sensitive metrics to DRE. For comparison purposes in Table 4, it was assumed that the differences of measured values for 100 kGy/h and 200 kGy/h were negligible and therefore are categorized together as lower dose rates.

Table 4. Summary on effect of dose rates for different evaluated test metrics.

Test Metric	Behavior of "Test Metric" from "low-to-high dose rates" at "highest absorbed dose"[1]		
	XLPE-1	XLPE-2	EPDM
Tensile Elongation at Break	-	-	Decreases
Mass Change	Decreases	Decreases	Increases
Yellowness Index	DRE Not Observed		
Carbonyl Index	Decreases	Increases	Decreases
Density	DRE Not Observed		
Indenter Modulus	DRE Not Observed		
Indenter Relaxation Time	DRE Not Observed		

[1]100 kGy/h and 200 kGy/h categorized as 'low dose rate' and 1800 kGy/h categorized as 'high dose rate'. 300 kGy is considered as "highest absorbed dose"

8. CONCLUSIONS

The objective of this report was to address one of the four cable aging knowledge gaps, dose rate effects, emphasized by (Fifield et al. 2018). Here, dose rate effects refer to gamma radiation-induced polymer degradation being a function of dose rate, in addition to total absorbed dose. The concern raised is that historical qualification conducted at higher dose rates to simulate service lifetime may underestimate insulation degradation that occurs at lower dose rates in service (NRC 2014).

In this report, nuclear cable insulation specimens of the most common types, XPLE and EPDM, from three of the most sourced manufacturers, were subjected to accelerated aging conditions at different dose rates of 100, 200 and 1800 Gy/h to total common dose of 100, 170, 300 kGy. To evaluate the effects of different dose rate, seven characterization methods were employed (elongation at break, mass change, yellowness index, carbonyl index, density, indenter modulus, and relaxation constant). It was observed that:

- The polymer insulation specimens exposed to gamma radiation do yellow with exposure, i.e., their yellowness index values increase compared to unaged samples. However, there was no significant difference observed with the yellowness index values for different dose rates for either of the material types, hence no DRE for YI.

- While few examples of previous research correlated the density of the polymer material as a quantity of degradation, this work showed that there is no observable difference in density values, for un-aged or gamma irradiated samples of XLPE and EPDM, and hence no DRE for density.

- Due to experimental issues, the elongation at break was measured successfully only for the EPDM specimen, and it is observed that the EAB decreases with increasing dose rate for EPDM.

- The relative mass change decreased for XLPE-1 and XLPE-2, whereas it increased for EPDM. This implies that there is DRE present in mass change, and it is dependent on material formulation.

- Based on the carbonyl index, DRE can be observed such that there is decrease in the carbonyl index for XLPE-1 and EPDM with dose rate, whereas there is a slight increase in CI with dose rate for XLPE-2.

- Significant changes due to DRE were not observed for indenter modulus or for relaxation constant for the material types investigated.

In terms of historical electrical cable qualification, the concern raised has been that rapid aging of electrical cable insulation to simulate lifetime service using higher dose rates may not accurately reflect aging in service at lower dose rates (NRC 2014). The findings from this work and cited previous work reveal that DRE are material dependent, even between similar material categories (e.g., XLPE). This may be due to the presence of additives, fillers and antioxidants introduced in different materials by various manufacturers, information that is proprietary to the manufacturer. In the case of the EPDM studied, degradation of ductility was observed to be greater at higher dose rate for the same total dose, indicating accelerated gamma aging to be more conservative than extended aging. Conclusions regarding the conservatism of historical qualification require additional consideration for specific materials and conditions in question.

The results of this study support the contention that, due to inherent limitations and uncertainties associated with prediction of cable remaining useful life from accelerated aging experiments, trending of installed cable insulation health status may be more practical and useful for safe and efficient cable aging management repair and replace decisions than lifetime prediction from historical qualification. The combination of material robustness demonstrated by the qualification process and ongoing monitoring of cable health status may to provide confidence in continued safe use of existing nuclear cables.

9. REFERENCES

Amin, A.-R. 2009. "Synergistic Effect of TNPP and Carbon Black in Weathered XLPE Materials." *Journal of Polymers and the Environment* 17 (4): 267-272. https://doi.org/10.1007/s10924-009-0148-5.

Burns, S. A. 2017. "Generating Reflectance Curves from sRGB Triplets." *arXiv preprint*. https://doi.org/10.48550/arxiv.1710.05732.

Fifield, L., Y. Ni, D. Li, A. Sriraman, A. Guzman, A. Ortiz, M. Spencer, M. Murphy, and A. Zwoster. 2022. *Inverse Temperature Effects in Nuclear Power Plant Electrical Cable Insulation,* PNNL-33296, Pacific Northwest National Laboratory, September 2022, https://lwrs.inl.gov/Materials Aging and Degradation/InverseTemperatureEffectsInNPP.pdf.

Fifield, L., M. Spencer, Y. Ni, D. Li, M. Pallaka, T. Bisel, A. Zwoster, and M. Murphy. 2020. *Sequential Versus Simultaneous Aging of XLPE and EPDM Nuclear Cable Insulation Subjected to Elevated Temperature and Gamma Radiation (Final Results),* PNNL-30041 Rev. 1, Pacific Northwest National Laboratory, June 2020, https://lwrs.inl.gov/Materials Aging and Degradation/Seq_vs_Sim_XLPE_EPDM_Cable_Insulation.pdf.

Fifield, L., A. Zwoster, and M. Murphy. 2018. *Initiation of Experimental Campaign to Address Knowledge Gaps Related to Simultaneous Thermal and Gamma Radiation Aging of Crosslinked Polyethylene and Ethylene-Propylene Rubber Cable Insulation,* PNNL-27987, Pacific Northwest National Laboratory, September 2018. https://doi.org/10.2172/1735758.

Gazdzinski, R. F., Denny, W.N., Toman, G.J., Butwin, R.T. 1996. *Aging Management Guideline Commercial Nuclear Power Plants - Electrical Cable and Terminations*, SAND96-0344, Sandia National Laboratories, September 1996, https://www.nrc.gov/docs/ML0311/ML031140264.pdf.

Gillen, K. T. 2020. "Importance of Synergism for Degradation of Elastomers in Combined Radiation Plus Temperature Environments." *Rubber Chemistry and Technology* 93 (1): 121-141. https://doi.org/10.5254/rct.19.80457.

Gillen, K. T., R. A. Assink, and R. Bernstein. 2005. *Nuclear Energy Plant Optimization (NEPO) Final Report on Aging and Condition Monitoring of Low-Voltage Cable Materials.* United States. https://www.osti.gov/biblio/875986

Gillen, K. T., and R. L. Clough. 1981. "Occurence and Implications of Radiation Dose-Rate Effects for Material Aging Studies." *Radiation Physics and Chemistry (1977)* 18 (3-4): 679-687. https://doi.org/10.1016/0146-5724(81)90191-6.

—. 1989. "Time-Temperature-Dose Rate Superposition: A Methodology for Extrapolating Accelerated Radiation Aging Data to Low Dose Rate Conditions." *Polymer Degradation and Stability* 24 (2): 137-168. https://doi.org/10.1016/0141-3910(89)90108-0.

—. 1992. "Rigorous Experimental Confirmation of a Theoretical Model for Diffusion-Limited Oxidation." *Polymer* 33 (20): 4358-4365. https://doi.org/10.1016/0032-3861(92)90280-a.

Gong, Y., J. Tang, X.-L. Yang, Z.-G. Yang, X.-Q. Shi, Y.-C. Xie, A.-H. Guo, and J.-F. Xu. 2019. "Effect of Irradiation Dose Rates on Ethylene-Propylene Rubber for Nuclear Cables." *Applied Surface Science* 484: 845-852. https://doi.org/10.1016/j.apsusc.2019.04.152.

Gryn'ova, G., J. L. Hodgson, and M. L. Coote. 2011. "Revising the Mechanism of Polymer Autooxidation." *Organic & Biomolecular Chemistry* 9 (2): 480-490. https://doi.org/10.1039/C0OB00596G.

Guadagno, L., P. Longo, M. Raimondo, C. Naddeo, A. Mariconda, V. Vittoria, G. Iannuzzo, and S. Russo. 2011. "Use of Hoveyda–Grubbs' Second Generation Catalyst in Self-Healing Epoxy Mixtures." *Composites Part B: Engineering* 42 (2): 296-301. https://doi.org/10.1016/j.compositesb.2010.10.011.

Hu, P., P.-P. Zhao, G. W. Zhang, and X.-H. Wang. 2016. "Thermal Properties of 60Co Irradiated Crosslinked High Density Polyethylene." *Solar Energy Materials and Solar Cells* 149: 55-59. https://doi.org/10.1016/j.solmat.2015.12.042.

Joskow, P. L. 2006. "The Future of Nuclear Power in the United States: Economic and Regulatory Challenges." MIT Center for Energy and Environmental Policy Research, December 2006. https://ceepr.mit.edu/wp-content/uploads/2023/02/2006-019.pdf.

Kochetov, R., T. Christen, and F. Gullo. "FTIR Analysis of LDPE and XLPE Thin Samples Pressed between Different Protective Anti-Adhesive Films." 2017. 2017 1st International Conference on Electrical Materials and Power Equipment (ICEMPE), 14-17 May 2017, Xi'an, China, https://doi.org/10.1109/icempe.2017.7982097.

Linnig, F. J., and J. E. Stewart. 1958. "Infrared Study of Some Structural Changes in Natural Rubber During Vulcanization." *Rubber Chemistry and Technology* 31 (4): 719-736. https://doi.org/10.5254/1.3542330.

Mitra, S., A. Ghanbari-Siahkali, P. Kingshott, S. Hvilsted, and K. Almdal. 2006. "An Investigation on Changes in Chemical Properties of Pure Ethylene-Propylene-Diene Rubber in Aqueous Acidic Environments." *Materials Chemistry and Physics* 98 (2-3): 248-255. https://doi.org/10.1016/j.matchemphys.2005.09.028.

NRC. 2014. *Expanded Materials Degradation Assessment (EMDA): Aging of Cables and Cable Systems (NUREG/CR-7153, Volume 5).* (NUREG/CR-7153, Volume 5). U. S. Nuclear Regulatory Commission, October 2014, https://www.nrc.gov/reading-rm/doc-collections/nuregs/contract/cr7153/v5/index.html.

Przybytniak, G., J. Boguski, V. Placek, L. Verardi, D. Fabiani, E. Linde, and U. W. Gedde. 2015. "Inverse Effect in Simultaneous Thermal and Radiation Aging of EVA Insulation." *Express Polymer Letters* 9 (4): 384-393. https://doi.org/10.3144/expresspolymlett.2015.36.

Reynolds, A., R. Bell, N. Bryson, T. Doyle, M. Hall, L. Mason, L. Quintric, and P. Terwilliger. 1995. "Dose-Rate Effects on the Radiation-Induced Oxidation of Electric Cable Used in Nuclear Power Plants." *Radiation Physics and Chemistry* 45 (1): 103-110, https://doi.org/10.1016/0969-806X(94)E0003-2.

Seguchi, T., K. Tamura, H. Kudoh, A. Shimada, and M. Sugimoto. 2015. "Degradation of Cable Insulation Material by Accelerated Thermal Radiation Combined Ageing." *IEEE Transactions on Dielectrics and Electrical Insulation* 22 (6): 3197-3206. https://doi.org/10.1109/Tdei.2015.004880.

Seguchi, T., K. Tamura, T. Ohshima, A. Shimada, and H. Kudoh. 2011. "Degradation Mechanisms of Cable Insulation Materials During Radiation-Thermal Ageing in Radiation Environment." *Radiation Physics and Chemistry* 80 (2): 268-273. https://doi.org/10.1016/j.radphyschem.2010.07.045.

Sidi, A., J. Colombani, J.-F. Larché, and A. Rivaton. 2018. "Multiscale Analysis of the Radiooxidative Degradation of EVA/EPDM Composites. ATH Filler and Dose Rate Effect." *Radiation Physics and Chemistry* 142: 14-22. https://doi.org/10.1016/j.radphyschem.2017.04.007.

Simmons, K. L., P. Ramuhali, D. L. Brenchley, J. B. Coble, H. M. Hashemian, R. Konnick, and S. Ray. 2012. *Light Water Reactor Sustainability (LWRS) Program – Non-Destructive Evaluation (NDE) R&D Roadmap for Determining Remaining Useful Life of Aging Cables in Nuclear Power Plants.* PNNL-21731, Pacific Northwest National Laboratory, September 2012. https://www.osti.gov/biblio/1133783

Subudhi, M. 1996. *Literature Review of Environmental Qualification of Safety-Related Electric Cables.* NUREG/CR-6384 Vol. 1, Part 2, U.S. Nuclear Regulatory Commission, April 1996. https://www.nrc.gov/reading-rm/doc-collections/nuregs/contract/cr6384/v2/index.html.

Tefferi, M., Z. Li, Y. Cao, H. Uehara, and Q. Chen. 2019. "Novel EPR-Insulated DC Cables for Future Multi-Terminal MVDC Integration." *IEEE Electrical Insulation Magazine* 35 (5): 20-27. https://doi.org/10.1109/mei.2019.8804331.

Troscianko, J., and M. Stevens. 2015. "Image Calibration and Analysis Toolbox – a Free Software Suite for Objectively Measuring Reflectance, Colour and Pattern." *Methods in Ecology and Evolution* 6 (11): 1320-1331. https://doi.org/https://doi.org/10.1111/2041-210X.12439.

Zhang, Y., Z. Wu, C. Qian, X. Tan, J. Yang, and L. Zhong. 2020. "Research on Lifespan Prediction of Cross-Linked Polyethylene Material for XLPE Cables." *Applied Sciences* 10 (15): 5381. https://doi.org/10.3390/app10155381.

Zhao, Q., X. Li, and J. Gao. 2007. "Aging of Ethylene–Propylene–Diene Monomer (EPDM) in Artificial Weathering Environment." *Polymer Degradation and Stability* 92 (10): 1841-1846. https://doi.org/10.1016/j.polymdegradstab.2007.07.001.

APPENDIX

Comparison of Elongation at Break due to DRE with Literature Data

The concern for Dose Rate Effects (DRE) was raised when it was recognized that the degradation of a polymer material may greater when the total dose is obtained at a lower dose rate than when the same dose is obtained at a higher dose rate (Reynolds et al. 1995; Gillen and Clough 1981). Such behavior is demonstrated in the schematic shown in Figure A1. However, the EAB results in this report for EPDM show the opposite behavior. Hence, further evaluation on EAB was performed with the literature.
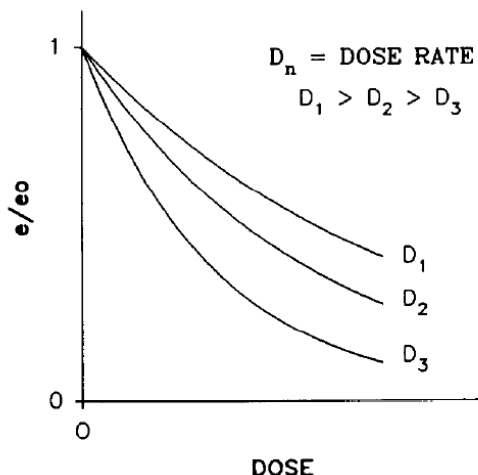

Figure A13: Schematic Illustration of the dose-rate effect (Reynolds et al. 1995)

In this section, the literature values for elongation at break (EAB) obtained at different dose rates as reported in SAND2005-7331 (Gillen et al. 2005) are compared to this work. This was done to further examine DRE on EAB, as EAB values were not available for all the specimens in this work.

It was observed that the polymer cable insulation materials examined in this report - XLPE-1, XLPE-2 and EPDM are similar to the materials reported in the SAND2005-7331 as XLPO-05 (Rockbestos Firewall III), XLPO-02 (Brand-Rex) and EPR-03 (Eaton Dekoron), respectively. Hence, the relative EAB values reported in the literature for these three materials are compared with our relative EAB values. Though similar in description to the materials evaluation herein, the materials studied in the previous work may be of different composition based, for instance, on year of manufacture. Aging conditions between the two sets of materials also varied. The aging and test conditions for the XLPO-05, XLPO-02 and EPR-03 are provided in SAND2005-7331. The Relative EAB % values for XLPO-05, XLPO-02 and EPR-03 materials are obtained with reference to their unaged specimen values reported in Table I-3 of SAND2005-7331. The Relative EAB % values for the XLPE-1, XLPE-2 and EPDM are calculated relative to the un-aged EAB values for the experiments performed in this report.

Table A5. Initial Elongation at Break % for materials in this report and in literature (Gillen et al. 2005)

This work (PNNL-34068)		SAND2005-7331	
Material	Initial Elongation EAB_i %	Material	Initial Elongation EAB_i %
XLPE-1	237	XLPO-05	300
XLPE-2	290	XLPO-02	310
EPDM	344	EPR-03	400

Figure A2 shows the relative EAB/EAB_i % values for XLPE-1 subjected to gamma radiation at a dose rate of 1800 Gy/h and XLPO-05, which was radiated at a dose rate of 210 Gy/h. Based on these results, it can be observed that DRE exists for the XLPE-1 or XLPO-05 material, as the degradation is higher at the lower dose rate.
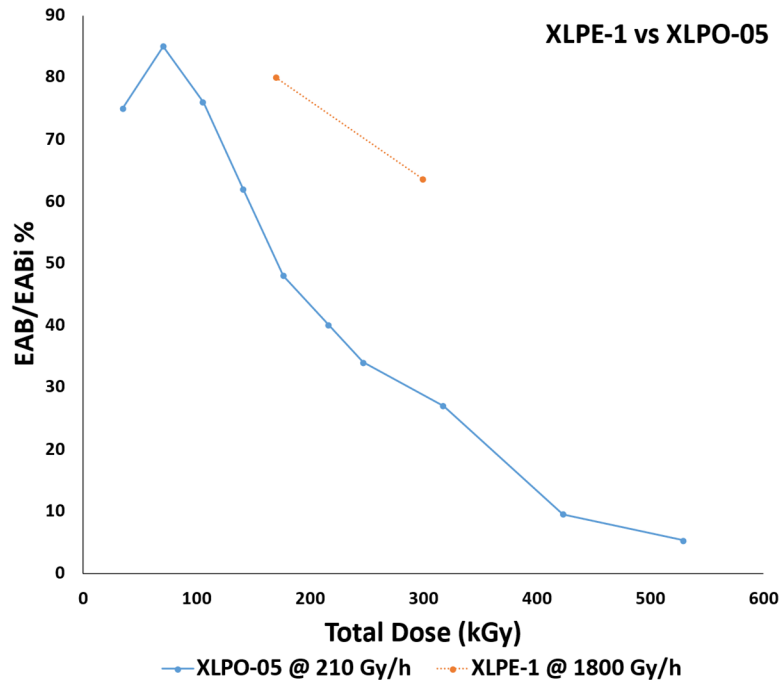

Figure A14: Average Relative EAB/EAB_i for XLPE-1 and XLPO-05 materials

The XLPE-2 material, considered in this report was aged at dose rates of 100, 200 and 1800 Gy/h and the XLPO-02 material was aged at 17, 124 and 210 Gy/h as shown in Figure A3. It can be observed that the degradation was higher in the lower dose rate cases for the XLPO-02 material and when compared with dose rate of 1800 Gy/h for the XLPE-2 material. However, due to limited data for the 100 Gy/h dose rate at the total dose of 300 kGy, conclusions cannot be drawn for the XLPE-2 material.
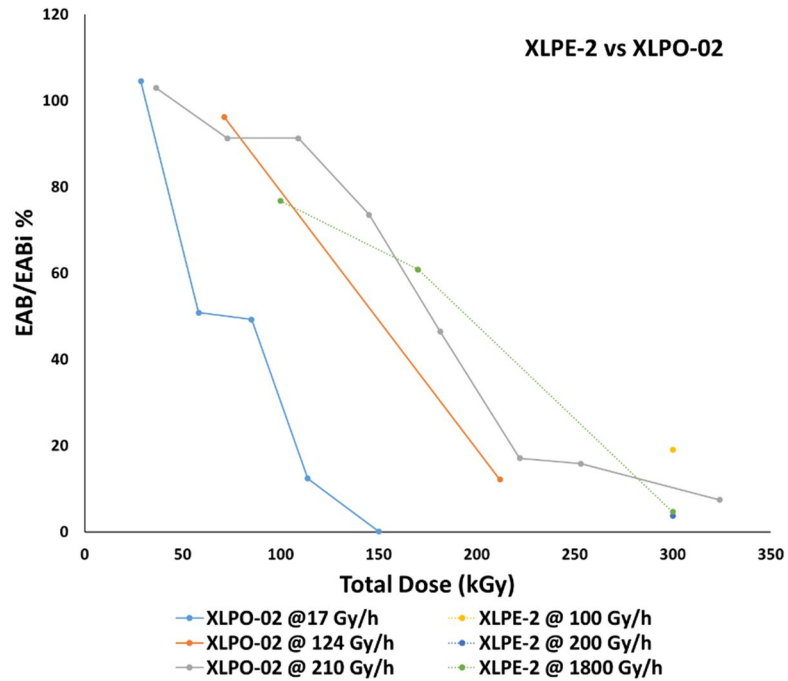
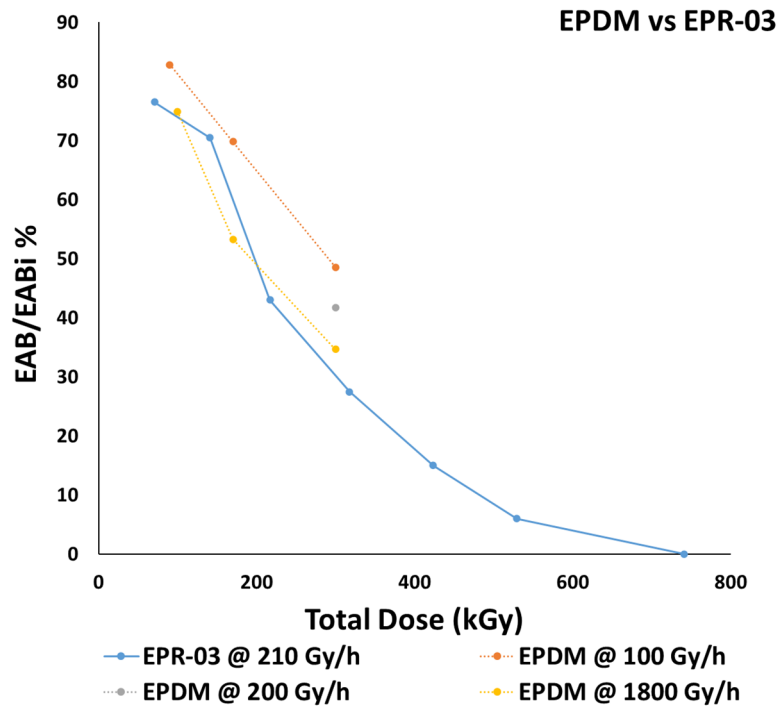Figure A15: Average Relative EAB/EAB$_i$ for XLPE-2 and XLPO-02 materials

Figure A16. Average Relative EAB/EAB$_i$ for EPDM and EPR-03 materials

The Relative EAB values for the EPDM material demonstrate that the degradation is higher at the higher dose rate rather than the lower dose rate, and with the data for EPR-03, the behavior is not conclusive.